

Appendix C

Method of approximate reconstruction of temporal and spatial dependence of a pulse moving past a finite sequence of probes

In the following discussion we present a general purpose method of analyzing a finite sequence of time signals $F_i(t)$ that consist of local measurements of real valued observables taken at the diagnostic ports of a linear accelerator device, with i being the port index. We describe an algorithm that can reconstruct an accurate approximation of the true space and time dependence of the given observable $F(z, t)$ in the regions between the points of measurement where diagnostic access is possible. We also present the conditions needed for this approximation to hold, and we

test the algorithm by directly comparing an analytically defined wave pulse to the reconstruction of the spatial discretization of the original known pulse. We find that for many realistic physical systems as few as three probe signals provide a good reconstruction of the true spatial distribution of the known wave pulse.

C.1 Sequential measurements of a moving pulse

The motivation for developing this type of interpolation originates with daily task of trying to comprehend and interpret each sequence of time signals in real time as the data comes in. After some experience with the raw signals, a sort of mental-interchange of space and time coordinates is possible to visualize; resulting in an intuitive appreciation of the accelerator dynamics and an approximate understanding of how a given observable varies in space. Of course, it is often difficult to fully communicate this understanding to others who are less familiar with the nuances of the particular system under consideration. In this paper we present an algorithm that produces a quantitative result that makes the accelerator dynamics easy to interpret. Below in fig. 1 is presented some sample data from the Compact Toroid Injector eXperiment (CTIX), where magnetized hydrogen plasma is accelerated past a sequence of three magnetic field probes. One problem that has been central to motivating this work has been the question of what is the exact magnetic geometry of the compact toroid plasma. Essentially, we would like to know what is the function $B(z, t)$ that describes the magnetic field as a function of axial position and time. A variety of other experimental observables are also measured at sequential positions and can benefit from this interpolation analysis. The details of the CTIX facility are explained in [ref,ref,ref] [fig 1 Bz signals at 57, 91, 142] A similar problem arises in video decompression schemes when trying to interpolate in time between actual frames of a video image, in order to reconstruct a better video at a higher frame rate.[ref,ref] The motion of distinct features within an image can be taken into account to predict where each feature will be at any intermediate time t , according to a quadratic model of its trajectory. In

in this problem the observables are vectors, and the details of any practical solution ultimately rely on some advanced image analysis. While the problem of one dimensional flow considered in this paper is in some sense a lower-dimensional special case of the motion-compensated interpolation used in video analysis, in which the space and time coordinates have been interchanged, it is worth formulating this application in a coherent and directly useable way. The algorithm we have developed can be broken down into two distinct sub-processes. The first process uses correlation functions of adjacent probe signals to calculate a set of time-of-flight correspondence maps that approximately track individual fluid elements as they pass by the probe positions. The second process takes this set of correspondence maps and uses it to create fluid element trajectories, and finally computes a unitary superposition of the adjacent real data to determine the interpolated value of the observable at intermediate positions along each trajectory. For example, these signals could be measuring a given component of the magnetic field at several axial positions as a function of time, or the average particle density, or light emission.

C.2 Lagrangian Interpolation Algorithm

This method can be simply described by the following general formula for the interpolated value of the observable $f(z, t)$ at position z between the i th and $(i+1)$ th real probes, which involves a unitary superposition of neighboring probe signals, evaluated at retarded and advanced times:

$$f(z, t) = w_i(z, t)F_i(t + \Delta t_i(z, t)) + (1 - w_i(z, t))F_{(i+1)}(t + \Delta t_{i+1}(z, t)) \quad (\text{C.1})$$

where w_i is a weighting factor (≤ 1) dependent on the fractional distance between the position z of and the positions of the real probes. Although w_i can in general depend on z and t , the simplest good implementation is actually independent of time, $w_i(z) = (z - Z_i)/(Z_{i+1} - Z_i)$ where Z_i is the position of the i th real probe, $i \in \{1, 2, \dots, (n-1)\}$. The function $F_i(t)$ is the time signal of the i th real probe, and $\Delta t_i(z, t)$, $\Delta t_{i+1}(z, t)$ are some delay functions that will need to be optimized

for best agreement with the approximately measured flow dynamics inferred from the time of flight between sequential probes. For fluid that is moving in the positive z direction, a given fluid element first passes by the lower probe at Z_i , then it passes through the value of z under consideration for interpolation, and lastly it passes the upper probe at Z_{i+1} . And so with the sign convention used in (C.1) we see that $\Delta t_i(z, t)$ will have negative values, while $\Delta t_{i+1}(z, t)$ will have positive values.

C.3 Estimation of Flow Field

Ideally we need to find the time-of-flight of each distinct fluid element as it travels between adjacent probes. To define distinct fluid elements we need to work with the group velocity of the wave pulse, and the most robust approach is to calculate the correlation function between adjacent probe signals

$$C_i(\Delta t) = \int F_i(t) F_{(i+1)}(t + \Delta t) dt$$

The peak of $C_i(\Delta t)$ occurs when Δt is equal to the time of flight of the pulse between the probes. This is a much better method than simply comparing the time of peak probe signals, which can produce erroneous results that are a combination of the group velocity and the phase velocity of any higher frequency modes within the pulse. The result of this step is a vector of time shifts Δt_i such that $C_i(\Delta t_i) = \max C_i(\Delta t)$, $i \in \{1, 2, \dots, (n-1)\}$.

Implementation The only challenge is establishing a good model of the fluid velocity $v(z_n)$ at each virtual probe position as a function of time. Finally, once $f(z, t)$ has been found it is then possible to resample the combined set of probe signals, real and virtual, to get F as a function of z , for each timeslice. This process of interpolation generates the function $F(z_n, t)$ from the measurements $F_1(t), F_2(t), \dots, F_n(t)$. It is standard to formulate this type of problem in terms of a flow function

$$\eta(\hat{x}, t)$$

C.4 Validity of Approximation

Test the algorithm by directly comparing an analytically defined wave pulse to the reconstruction of the spatial discretization of the original known pulse. Accurate for longest wavelength modes. Timescale of interpolation is much smaller than Resistive Diffusion timescale. Numeric simulation test shows what the fastest measurable mode is ... numerical reconstruction of an analytical test function

C.4.1 First order velocity error

We need to find the error in the velocity curve of the CT-pushing field interface (CT back edge), since this will have an effect on the entire reconstruction. The key idea is that will be some time error Δt in the measurement of the time that the CT back passes each probe position, and this error is dependent on the random fluctuation of the signal level, and inversely proportional to the slope of the signal at the crossing time. $\Delta t = \frac{1}{m} \Delta B_z$. First we need to estimate the signal fluctuation level. Here we will investigate the high frequency noise in the B_z signal as being the source of any errors in computing the velocity of the CT as a function of time. We will define the signal fluctuation to be the maximum absolute value of the residual of the B_z signal after subtracting off a smoothed version of the original signal.

$$\Delta B_z = \max |B_z(t) - \text{smoothed}(B_z(t))|$$

However, the result of this is dependent on exactly how much smoothing is done. To provide an objective criterion for sufficient smoothing, and thereby yield uniform results in this analysis, we will adopt the following procedure to implement the smoothing. The primary concern with this procedure is that it smoothes enough, but not too much. The fluctuations that we identify as noise in our B_z signals typically exhibit a rapid change from positive to negative slope over a short interval of time. And so the “true” signals (as we conceptualize them) that lie underneath the noise will not have this “jumpy” character to them. As a reasonable measure of this “jumpyness” factor we

can consider the first time derivative of the partially smoothed signal S_i , and then multiply it by a weighting factor determined by the duration that the signal is near that value of time-slope. The result is a function of time

$$jump(t) = \frac{1}{Duration(slope)} \cdot \frac{dS_i(t)}{dt}$$

Here, the term $Duration(slope)$ is simply the time between zero crossings of the time derivative, and it measures (in a piecewise fashion) the duration that the signal has either positive or negative slope. The reason for dividing by the duration of same-sign slope is that the physically real signal may have large slopes, but it will typically maintain this slope for some extended period of time; whereas noise will change the sign of its slope every few digitization steps. As the original signal is iteratively smoothed, the noise will be removed, and the maximum absolute value of $jump(t)$ of the i th partially smoothed signal S_i , will fall monotonically. Let us call this jumpiness parameter $\xi = \max |jump(t)|$. The smoothing process should stop when ξ falls below some small predetermined value ξ_{stop} , which should be in agreement with estimates of the signal to noise ratio for the probe signals. Approximately, $(1 - \xi_{stop}) \sim (signal/noise)$. For example, here is the Bz 57, 91, and 142 signals for shot ?. With a value for the smoothing limit of $\xi_{stop} = 0.01$ we will tabulate the estimated signal error ΔB_z , and a corresponding arrival-time error $\pm \Delta t$ for each probe. Lastly we list the relative error of the final velocity of the CT, derived from the maximum possible error considering all possible sign combinations for each of the arrival time errors. Note that if you had a set of three new arrival times that were all shifted in the same direction (either + or -) by the same amount Δt , then the calculated final velocity with these "errors" would be exactly the same as the true final velocity. Only if there is some asymmetric distribution of positive or negative errors, will the resulting error of the final velocity reach its maximum value. Here we list this worst case velocity error as an upper bound.

C.4.2 Constraints on the amplitude of undetectable transient pulses

In order to estimate the reliability of this reconstruction method we need to carefully consider the worst possible errors that could in the space between consecutive probes. We will consider errors that are as large as the mathematics of the algorithm allow, with no concern initially for the physical limitations on such errors. The end result of this analysis is a constraint in the form of an uncertainty relation between the duration and spatial extent of any undetected transient pulse-like modulations of the field occurring in the unmeasured region between the probes. This will provide a solid upper limit to the total error of the reconstruction. Since the probes themselves yield extremely accurate and reproducible measurements of the field quantities in the immediate vicinity of the probe locations, there is very little error due to global fluctuations, since these would be detected simultaneously by multiple probes. Instead, the real cause for concern are *transient fluctuations*, that cause error because they are short enough in duration and spatial extent, and happen to occur deep enough into the empty space between probes so that they go undetected, and consequently the algorithm has no ability to include their existence in the reconstructed waveform.

It is tractable and informative to consider transient pulses that have a Gaussian form in space and time (z, t) such as

$$\mathcal{F}(z, t) = A e^{-\left(\frac{t - t_p}{\tau}\right)^2} e^{-\left(\frac{z - vt}{L}\right)^2}, \quad (\text{C.2})$$

here, A is the amplitude of the pulse, τ is the characteristic rise/decay time of the pulse, ie its duration, L is the characteristic spatial extent, t_p is the time at which the pulse reaches its peak value, and v is the pulse group velocity, which we will assume is approximately the average fluid velocity. To measure the damage this pulse could do to our reconstruction, we need the envelope of the pulse as a function of position z , which is the maximum value of the pulse at a fixed z , over all values of time.

First we find, for each z , the value of t maximizes $\mathcal{F}(z, t)$. For positive-valued Gaussians like we are considering, there is a finite maximum value but no minimum value for finite (z, t) . The maximum occurs when $\partial\mathcal{F}/\partial t = 0$,

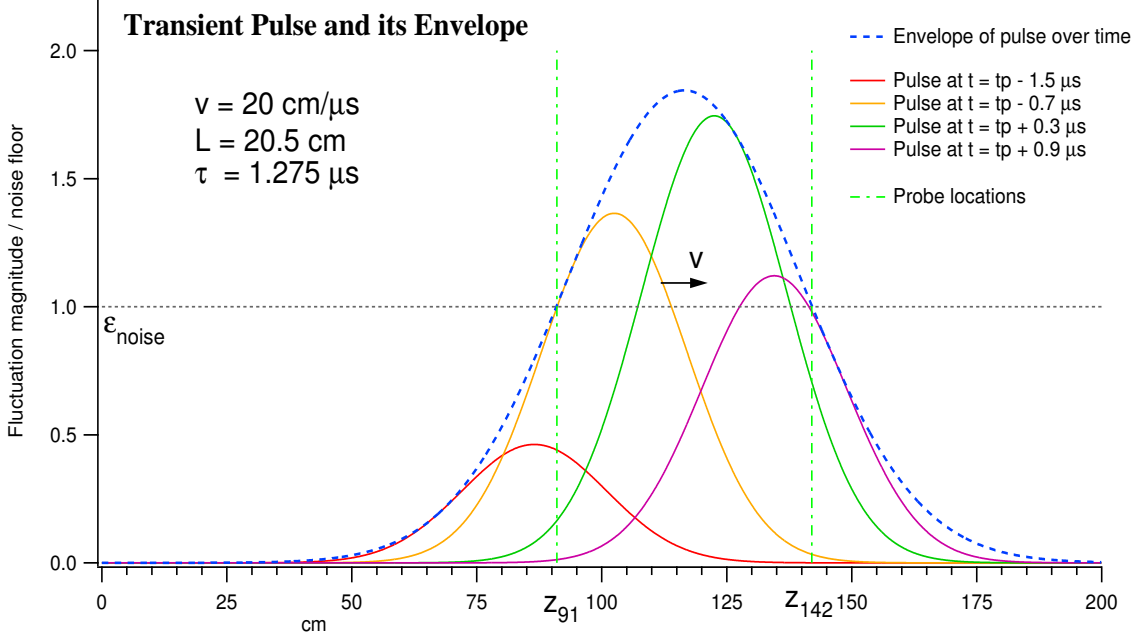


Figure C.1: Transient pulse at various times and its time-envelope as a function of axial position.

$$\frac{\partial \mathcal{F}}{\partial t} = -\mathcal{F}(z, t) \left(\frac{2}{\tau} \left(\frac{t - t_p}{\tau} \right) - \frac{2v}{L} \left(\frac{z - vt}{L} \right) \right)$$

And so the maximum occurs when

$$\frac{t - t_p}{\tau^2} - \frac{v(z - vt)}{L^2} = 0$$

$$\text{or} \quad t \left(1 + \frac{v^2 \tau^2}{L^2} \right) = t_p + \frac{v^2 \tau^2 z}{L^2}$$

Now, to clarify the algebra, let us define a dimensionless parameter $\kappa = v\tau/L$, and we see that for a fixed z the pulse reaches a maximum value at time

$$t = t_{max}(z) = \frac{t_p + \frac{\kappa^2 z}{v}}{(1 + \kappa^2)}$$

The envelope is given by $\mathcal{F}_{env}(z) = \mathcal{F}(z, t_{max}(z))$, which simplifies to

$$\mathcal{F}_{env}(z) = A e^{-\left(\frac{z - vt_p}{L\sqrt{1+\kappa^2}} \right)^2}.$$

Restated in terms of τ , (using $L\sqrt{1+\kappa^2} = \sqrt{L^2+v^2\tau^2}$), this is

$$\mathcal{F}_{env}(z) = A e^{-\left(\frac{z-vt_p}{\sqrt{L^2+v^2\tau^2}}\right)^2}. \quad (C.3)$$

In order for this pulse to be undetected by neighboring probes located at z_A and z_B we would need the pulse envelope to be less than some noise floor ϵ_{noise}

$$\mathcal{F}_{env}(z_A) < \epsilon_{noise} \quad \text{and} \quad \mathcal{F}_{env}(z_B) < \epsilon_{noise} \quad (C.4)$$

where ϵ_{noise} is the determined by statistical fluctuations that are present in an ensemble of measured signals under equivalent experimental circumstances. It does not have to be restricted to just the electrical noise present in the probe diagnostics, but could include actual MHD modes in the plasma that constitute random deviations away from the average waveform of the probe signals. It is at least conceptually possible that occasionally these real fluctuations would occur at a larger than normal amplitude and in a transient fashion between the probes, and thus go undetected. In the worst case scenario the peak of the transient pulse would occur at exactly the half-way point between consecutive probes, thereby allowing the largest possible amplitude allowable by (C.4). From this (unlikely) situation, we could make the most conservative estimate for the accuracy of this reconstruction method. The true accuracy should only be better than what we find here. The worst case is when $vt_p = z_{mid} = \frac{1}{2}(z_A + z_B)$, and so let $\Delta L_{probe} = 2(z_B - z_{mid})$. Then condition for nondetection is

$$A e^{-\left(\frac{\Delta L_{probe}}{2\sqrt{L^2+v^2\tau^2}}\right)^2} < \epsilon_{noise} \quad (C.5)$$

And the maximum possible undetectable amplitude is constrained by

$$A < \epsilon_{noise} e^{\frac{\Delta L_{probe}^2}{4(L^2+v^2\tau^2)}} \quad (C.6)$$

This maximum possible amplitude is plotted in fig (C.4.2) as a function of fluctuation duration and spatial extent (τ, L) using parameters typical for the CTIX experiment. Using this result we can make statements regarding an upper bound of the error of the reconstruction method, such as:

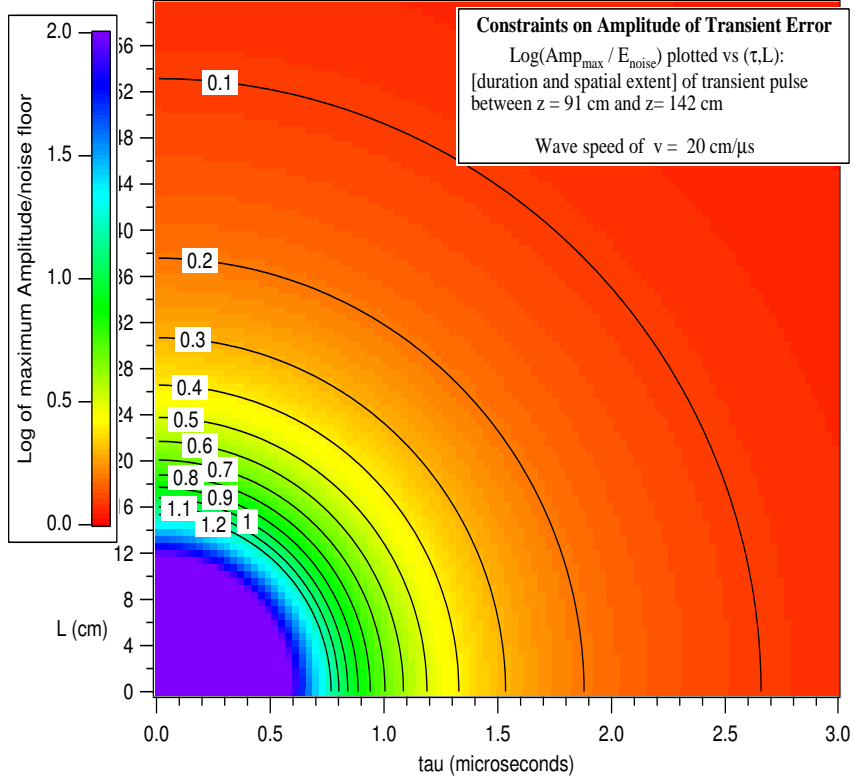


Figure C.2: Log (base 10) of the maximum possible amplitude of undetected transient pulses, plotted as a function of pulse duration and spatial extent.

For an average fluid velocity of $v = 20 \text{ cm}/\mu\text{s}$ in the region between $z_A = 91 \text{ cm}$ and $z_B = 142 \text{ cm}$, if there exists an undetected transient pulse that spans the space between the probes, and exists for at least the transit time between probes [$2L = 51 \text{ cm} \Rightarrow L = 20.5 \text{ cm}$ and $2\tau = (51/20)\mu\text{s} \Rightarrow \tau = 1.275\mu\text{s}$], (see fig C.4.2) then the amplitude of the pulse can be no larger than

$$A_{max} = 1.84493 \cdot \epsilon_{noise}$$

For pulses that are significantly shorter in duration and extent, the upper limit on amplitude becomes much larger than this example. In fact, formula (C.6) goes to ∞ in the limit of zero pulse length and duration. Ultimately however, this does not cause any serious problems if our goal is to reconstruct the average waveform of the field moving past a set of probes, where we care about a spatial resolution of several cm, and temporal resolution of a few μs . Also, there is a mitigating factor involving the probability of these hypothetical high-amplitude events. If we take the noise floor to be the expectation value of the natural fluctuations \mathcal{F} that occur with the plasma, $\epsilon_{noise} = \langle \mathcal{F} \rangle$,

then we can use Markov's inequality [ref] to bound the probability that a high-amplitude event will occur during any given shot. Let \mathcal{F} be a nonnegative random variable; then for any amplitude of fluctuation $A > 0$, the probability that \mathcal{F} will exceed A is bounded according to

$$P(\mathcal{F} > A) \leq \frac{\langle \mathcal{F} \rangle}{A}$$

For example, the probability that a fluctuation will exceed 100 times ϵ_{noise} , is at the very most 1/100. And so, although high amplitude errors are possible, they are constrained by basic probability laws to be correspondingly rare occurrences. Alternatively, if there is some physical reason for some finite upper bound on A , such as conservation of energy perhaps, then we can restate equation (C.6) in the form of an uncertainty relation

$$L^2 + v^2\tau^2 < \frac{\Delta L_{probe}^2}{4 \ln\left(\frac{A}{\epsilon_{noise}}\right)} \quad (C.7)$$

We see that if $A < \epsilon_{noise}$ then L and τ are unconstrained, which agrees with the fact that small amplitude fluctuations have already been included in our definition of ϵ_{noise} . But as A becomes larger, the region of spacetime with a significant reconstruction error must become smaller and smaller, and its occurrence becomes increasingly improbable. Lastly, for some fixed $A > \epsilon_{noise}$, we see that there is a trade-off between the spatial extent and the duration of undetectable pulses, and that this relationship depends on the fluid velocity and the distance between consecutive probes. The best reconstruction occurs when consecutive probes are closely spaced, and there is a high flow velocity.